Atmospheric Research 99 (2011) 377–390

Contents lists available at ScienceDirect

Atmospheric Research

journal homepage: www.elsevier.com/locate/atmos

Cloud-to-ground lightning and Mesoscale Convective Systems

Enrique V. Mattos *, Luiz A.T. Machado

National Institute for Space Research — INPE, Center for Weather Forecast and Climate Studies — CPTEC, Rodovia Presidente Dutra, km 40, Cachoeira Paulista-SP 12630000, Brazil

ARTICLE INFO

Article history:
Received 23 May 2010
Received in revised form 2 November 2010
Accepted 8 November 2010

Keywords:
Lightning
Mesoscale Convective System
Cloud microphysics
Nowcasting

ABSTRACT

This work analyzes some physical and microphysical properties of Mesoscale Convective Systems (MCSs) and cloud-to-ground lightning. Satellite data from the GOES-10 infrared and NOAA-18 and TRMM microwave channels and lightning information from the Brazilian lightning detection network (BrasilDAT) were utilized for the period from 2007 to 2009. Based on an automatic MCSs detection method, 720 MCSs life cycles were identified during the period and in the region of study, with a lightning detection efficiency of over 90%. During the diurnal cycle, maximum electrical activity occurred close to the time of maximum convective cloud fraction (18 UTC), and 3 h after the maximum normalized area expansion rate. Diurnal cycles of both properties were modulated by diurnal heating, and thus could be used to monitor diurnal variability of lightning occurrence. The electrical activity was more intense for the widest (Pearson's correlation of 0.96) and deeper (Pearson's correlation of 0.84) clouds, which reached 390 km size and 17 km maximum cloud top height. Area growth during the initial phase of MCSs exerted a strong influence on their size and duration, and thus also showed a potential for defining the possibility of electrical activity during their life cycle. The average lightning life cycle exhibited a maximum close to MCSs maturation, while the maximum average lightning density occurred in the MCSs initial life cycle stage. The growth rate of electrical activity during the early stages can indicate the strength of convection and the possible duration of systems with lightning occurrence. Strong condensation processes and mass flux during the growth phase of the systems can provide favorable conditions for cloud electrification and lightning occurrence. A comparison of high microwave frequencies with lightning data showed a strong relationship of vertically integrated ice content and particle size with lightning occurrence, with Pearson's correlation of 0.86 and 0.96, respectively. The polarization difference in the 85 GHz channel showed that electrical activity increases linearly with polarization reduction, associated with a high value of Pearson's correlation coefficient (above 0.90). This suggests that regions with more intense electrical activity are predominantly located in areas with a high concentration of larger ice particles that are vertically oriented, due to the existence of intense updrafts and the electric field. These results demonstrate the potential use of thermodynamic, dynamic and microphysical characteristics for analyzing thunderstorms severity, and as additional information for nowcasting and monitoring electrical activity over large regions that lack ground-based lightning sensors.

1. Introduction

The important role performed by Mesoscale Convective Systems (MCSs) in weather and climate has been investigated in studies of many regions, including Africa (Machado et al., 1993; Laing and Fritsch, 1993a; Laing et al., 1999; Schwendike et al., 2010; DeLonge et al., 2010), Australia (James, 1992), Asia (Miller and Fritsch, 1991; Laing and Fritsch, 1993b; Jain et al., 2010), Europe (Laing and Fritsch, 1997; Morel and Senesi, 2002), United States (US, Maddox, 1980; Rodgers et al., 1983; Fritsch et al., 1986; Kane et al., 1987; Tollerud and Collander, 1993; Anderson and Arritt, 1998; Ashley et al., 2003; Cohen, et al., 2007) and South America (SA, Velasco and Fritsch, 1987; Machado et al., 1998; Torres and Nicolini, 1999; Laing and Fritsch, 2000; Carvalho et al., 2002; Ferreira et al.,

* Corresponding author. Tel.: +55 12 31869523; fax: +55 12 31869291.
E-mail address: enrique.mattos@cptec.inpe.br (E.V. Mattos).

0169-8095
doi:10.1016/j.atmosres.2010.11.007

2003; Machado and Laurent, 2004; Salio et al., 2007; Durkee and Mote, 2009). The common aspect noted in these works is the efficiency of the MCSs in producing most of the precipitation in the tropics and in the summer in mid-latitudes, and also their association with severe weather conditions (lightning, intense precipitation, hail, strong winds, and flooding) in various regions of the world.

The southeast region of SA is known for having the most intense MCSs and lightning occurrence in the world (Nesbitt et al., 2000; Zipser et al., 2006). This occurs for the most part in spring and summer between 15°S and 30°S. However, Conforte (1997) confirmed that in SA, the highest Mesoscale Convective Complex (MCC) frequency is during spring (39%), followed by autumn (27%), summer (22%) and winter (12%). This region also is characterized by an average maximum temperature of around 24 °C during spring and summer and annual average precipitation of 2000 mm. For different seasons, MCSs formation on the continent is observed predominantly during the afternoon and the beginning of nighttime, reaching maximum extension during morning and dissipating around noon (Nicolini et al., 2002; Salio et al., 2007; Durkee and Mote, 2009). This life cycle reveals a strong dependence of MCSs formation on the valley nocturnal circulation (valley-mountain circulation associated the Andes Mountains) and humidity flux from the Amazon region transported by the Low-Level Jet (LLJ). However, gravity waves forced by the Andes, approaching cold fronts from southern Brazil and the South Atlantic Convergence Zone (SACZ) may also contribute to MCSs formation. Moreover, local factors such as the sea breeze and topography (such as the Mar and Mantiqueira Mountains) in eastern São Paulo state are important local factors capable of intensify severe weather in this region. Indeed, the conceptual model proposed by Marengo et al. (2004) suggests that humidity from the Amazon transported by the (LLJ) on the east of the Andes Mountain is the major energy source for the MCSs formation in southern Brazil during the summer, while in the winter it is humidity from the ocean associated with the South Atlantic Subtropical High. MCSs formation associated with coupling between synoptic and sub-synoptic mechanisms has been also confirmed by other studies realized by Marengo et al. (2002), Vera et al. (2006) and Salio et al. (2007) in SA and by Bonner (1968) in the US.

In addition, a number of studies have been conducted around the world on the relationship between cloud-to-ground (henceforth referred to as CG) lightning parameters and the variation of MCSs properties (dynamic, thermodynamic and microphysical parameters) during the life cycle (Mazur and Rust, 1983; Goodman and MacGorman, 1986; Williams et al., 1989; Rutledge et al., 1990; Keighton et al., 1991; Hunter et al., 1992; Petersen and Rutledge, 1992; Holle et al., 1994; Bateman et al., 1995; Bluestein and MacGorman, 1998; MacGorman and Morgenstern, 1998; Parker et al., 2001; Zhou et al., 2002; Liu et al., 2009; Tadesse and Anagnostou, 2009; Lima and Gomes, 2009). However, there are relatively few studies which relate CG lightning with cloud properties estimated from orbital sensors. The understanding of the relationship of changes in MCSs morphological and radiative properties with the intensification of convection and electrical activity would contribute to nowcasting of extreme weather events. The factors responsible for the thunderstorm electrification are not yet completely understood. Nevertheless, it has been accepted that collision between ice particles (ice crystals and hail) and super-cooled water is an important process for cloud electrification (Reynolds et al., 1957; Saunders, 1993). Non-inductive charging process has suggested that charge centers formed inside the cloud can produce an intense electric field (hundreds of kV/m) capable of breaking the dielectric rigidity of the air and driving the formation of electric discharges (Baker and Dash, 1989; Keith and Saunders, 1990; Tsenova et al., 2009).

Information from geostationary satellites thermal infrared window channels (IR, 10.2–11.2 μm) and radar have revealed prominent characteristics of the tops and organization of clouds associated with severe convection. Through a study of lightning activity evolution in two squall lines in the US and Asia, Mazur and Rust (1983) found that the maximum lightning density was near the leading edge of precipitation. It was also observed that shorter discharges predominate during the MCSs development stage and diminish or cease in the dissipative stage. Goodman and MacGorman (1986) showed that half of MCC observed over Oklahoma caused damages associated with lightning, which is most frequent between the development and mature stages of the systems. On the other hand, Williams et al. (1989), comparing lightning type and thunderstorm convective state in the US, found that intra-cloud activity dominates in the early cloud stage and is followed by predominant CG lightning occurrence. Nielsen et al. (1994) noted that positive CG lightning is dominant when the squall line is developing, negative during the period of strongest convective intensity and highest thunderstorm tops, and positive in the demise stage. Consistent with these results, Parker et al. (2001) verified that for three distinct middle-latitude MCSs, maximum CG lightning, both positive and negative, occurred before maximum system size. Rutledge et al. (1990), documented these same characteristics of positive CG lightning in MCSs, while the work of Liu et al. (2009) on hailstorms in China added that positive CG lightning dominates during most of the life cycle. Recently, Tadesse and Anagnostou (2009), using an automatic cloud tracking method, showed that the majority of systems with lightning have a duration of an hour longer than the others, in addition to exhibiting more intense electrical activity close to the maturation stage. Over the southern region of Brazil, Lima and Gomes (2009) analyzed three MCSs using a semi-automatic method and verified that the CG lightning maximum was close to maturation and associated with intense convection. The work of Machado and Laurent (2004) suggested that this life cycle phase corresponds to the moment of maximum high-level divergence and a decrease in the condensation rate, that is, the moment in which maximum convective cloud cover is achieved.

Clouds with low top temperatures have been primarily observed in regions of more intense electrical activity (Williams, 1985; Goodman et al., 1988; Ushio et al., 2001; Dotzek et al., 2005; Scofield et al., 2005; Altaratz et al., 2010). Williams (1985) observed that the lightning rate is a function of the fifth power of the cloud height, while Ushio et al. (2001) verified that the relationship has approximately exponential global behavior for winter/summer in the extratropics and ocean/continent in the tropics. Recently, Altaratz et al. (2010)

observed that during the dry season in the Amazon region, the quantity of return strokes increased as a function of the decrease in cloud top pressure (an approximately linear relationship) and increase in the cloud convective fraction (an approximately exponential relationship). For cloud top temperature, Goodman et al. (1988) found an increased lightning occurrence for temperatures below approximately 200 K, while Dotzek et al. (2005) observed a threshold of 203 K below overshooting tops with a V shape. Machado et al. (2009) showed that penetrating clouds are associated with electrical discharges and that there is an increased probability of CG electrical discharges with an increase in the difference in brightness temperature (T_B) between the infrared window and water vapor channels. Despite the different limits found in various regions, a common characteristic is the existence of a high correspondence between the average cloud top temperature of the MCSs in the IR and lightning occurrence.

Many studies using cloud electrification models have shown the existence of an interdependent relationship of electrical activity with ice particle size, concentration, and phase (Keith and Saunders, 1990; Mitzeva and Saunders, 1990; Baker et al., 1995; Miller et al., 2001; Tsenova et al., 2009), availability and distribution of super-cooled liquid water droplets (Saunders et al., 1991) and impact velocity of the ice particles (Mitzeva and Saunders, 1990; Brooks et al., 1997). However, a smaller number of studies have characterized this relationship using satellite microwave estimates. Keith and Saunders (1990) and Miller et al. (2001) used thunderstorm numerical modeling and observational data to show that the amount of charge transferred in the collisions between ices particles can depend nonlinearly on size. In addition, some studies have shown that increased lightning occurrence tends to be associated with an increase in the thunderstorm ice content (Baker et al., 1995; Blyth et al., 2001). The work of Petersen et al. (2005) suggested that, on the global scale, the relationship between ice content and lightning is approximately linear and invariable over continental, oceanic and coastal regions. On the other hand, the results of Spencer et al. (1989) and Prigent et al. (2001) have suggested that the orientation (vertical or horizontal) of ice particles can be investigated using the difference in T_B at 85 GH (T_{BV}–T_{BH}). They verified that more negative (positive) values indicate regions with more intense (less intense) thunderstorm convection. Similarly, Prigent et al. (2005), through a radiative transfer model and coincident information from the Tropical Rainfall Measuring Mission (TRMM) Microwave Imager (TMI) and the Lightning Imaging Sensor (LIS) on board TRMM, found that 50% of the cases over land with T_{BV}–T_{BH} close to or below 0 K were associated with lightning detection. The results have suggested that such polarization differences can be explained by relatively large and non-spherical particles that are mostly vertically oriented.

This work investigates the physical relationship of MCSs dynamic, thermodynamic and microphysical parameters with CG lightning occurrence using infrared and passive microwave channel information from satellites and lightning information obtained from ground based sensors. In this way, the potential of these parameters as indicators of severity and for prediction of electrical activity will be evaluated.

Section 2 describes the CG lightning and satellite data used and the methodology employed in this work. Section 3 presents diurnal cycle results and the relationships of the life cycle and physical and microphysical properties with CG lightning electrical activity. Finally, conclusions are presented in Section 4.

2. Data and methodology

2.1. The BrasilDAT network

The CG lightning data used in this study were provided by the Brazilian lightning detection network (BrasilDAT). BrasilDAT operates at Low Frequency (LF) and Very Low Frequency (VLF), and is composed of 47 sensors covering the south and southeast regions and part of the north e midwest of Brazil. Sensors using the Lightning Position and Tracking System (LPATS) and Improved Accuracy Using Combined Technology (IMPACT) technologies were employed. The combination of the geometric distribution with the technology utilized by the sensors results in an average precision of 500 m in locating CG lightning sources and a detection efficiency of 90% in some parts of the country (more details about the BrasilDAT network can be found in Pinto et al., 2007 and Naccarato and Pinto, 2009). The BrasilDAT data employed consists of location, date and time of CG lightning occurrences for the period from May 2007 to August 2009 over an area centered in the state of São Paulo, demarcated by longitudes 53 °W to 44 °W and latitudes 26 °S to 19 °S. This area was chosen as the standard for the study, because it is concentrated in the region of Brazil with the best and most homogeneous lightning coverage, resulting in a detection efficiency of over 90%. Fig. 1 shows the study area, indicated by the rectangle in bold, and the sensors located in this region, as well as the detection efficiency contour lines.

2.2. Infrared satellite data

T_B data from IR (10.2–11.2 μm) channel images from the Geostationary Operational Environmental Satellite (GOES-10) satellite were employed to determine the physical properties of the MCSs. These data were obtained and processed by Center for Weather Forecast and Climate Studies (CPTEC) which belongs to the National Institute for Space Research (INPE). The images were obtained in satellite projection and were reprojected to a rectangular projection covering all of SA for the period from May 2007 to August 2009, with temporal resolution of 15 min and spatial resolution of 4 km (sub-satellite point). These satellite images were assimilated by the Forecast and Tracking of Active Convective Cells (ForTraCC) algorithm in order to track the MCSs life cycle for the period mentioned earlier.

ForTraCC is an algorithm presented by Vila et al. (2008) that determines the trajectories and life cycle of these systems through successive IR images, based on morphological characteristics and superposition of areas between the images. A minimum size of 90 pixels (1440 km^2) and thresholds of 235 K and 210 K were defined in order to detect MCSs and Convective Cells (CC), respectively. This procedure produces a time series of MCSs physical properties (morphological and radiative characteristics) through their life cycle, such as: location, size, normalized area expansion rate, average and minimum brightness temperature, convective fraction, eccentricity,

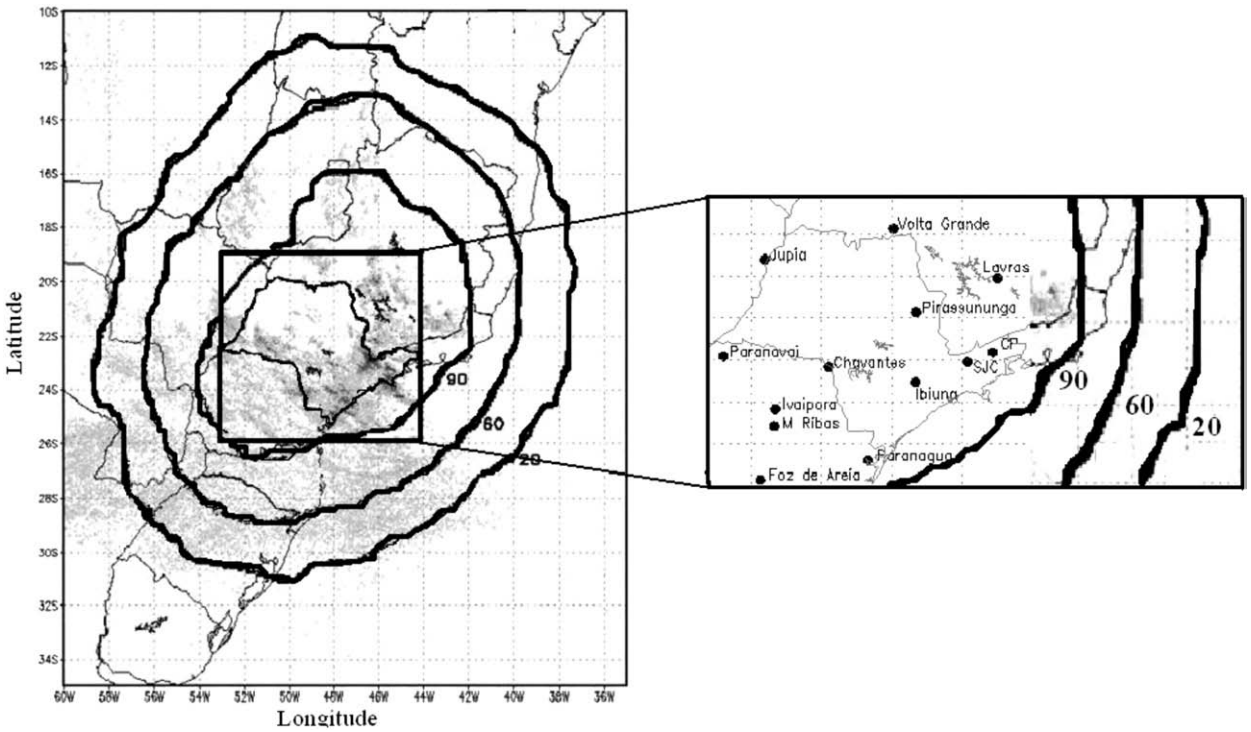

Fig. 1. Study region, location of BrasilDAT sensors inside this region and contour lines of CG lightning detection efficiency within 20, 60 and 90%. Adapted from Naccarato and Pinto (2009) and Machado et al. (2009).

inclination angle, and other parameters (more details in Machado et al., 1998). Only MCSs that passed over the state of São Paulo at some point in their life cycle were selected, with 16,520 systems identified during the study period. For each moment in the system life cycle, lightning occurrences were counted from 7.5 min before until 7.5 min after the image time. Statistical analyses were conducted in order to understand the diurnal cycle and to obtain relationships between physical properties and CG lightning. The dispersion analyses considered Pearson's correlation coefficients (R) and p-values (pv) with a significance level of 0.01.

The MCSs life cycle study was conducted considering only systems that: (1) initiated spontaneously (that is, that did not originate as the result of a systems split) and ended by dissipation (that is, did not end by merging with other systems) in the interior of the study area and (2) had few missing images (less than half the total lifetime). The first limitation assured that initial growth of the system was due to its internal dynamics and that its lifetime was representative of the entire lifetime (as discussed by Machado and Laurent, 2004). In addition, it assured that the systems were always located over an area with lightning detection efficiency that was constant and over 90%. In this way, 420 systems were identified with lightning (henceforth denominated thunderstorms) and 300 without lightning (henceforth denominated storms). It should be remembered that this work only considered cloud-to-ground discharges, and hence intra-cloud (IN) and cloud-to-cloud (CC) discharges were not considered. Thus, the specific denomination of storms and thunderstorms in this study was based only on the CG lightning condition.

2.3. Passive microwave satellite data

The estimations of ice particle effective diameter (D_e) and Ice Water Path (*IWP*) were made using an inference algorithm similar to that presented by Zhao and Weng (2002). The processing of this model was accomplished using the T_B from the 23 GHz and 31 GHz channels of the Advanced Microwave Sounder Unit-A2 (AMSU-A2) sensor and the 89 GHz, 157 GHz and 183.3 ± 1 GHz channels of the Microwave Humidity Sounder (MHS) sensor on board the National Oceanic and Atmospheric Administration (NOAA-18) satellite. These data were received by CPTEC/INPE and cover the period from January 2007 to September 2009. The parameterizations for estimating the values of D_e and *IWP* are determined by combining empirical and statistical methods similar to those presented by Zhao and Weng (2002), and can be expressed as

$$D_e = a_0 + a_1 r + a_2 r^2 + a_3 r^3 \quad (1)$$

and

$$IWP = \mu D_e \rho_i (\Omega_{89or157} / \Omega_N), \quad (2)$$

where a_0, a_1, a_2 and a_3 are the regression coefficients, which depend on the ice particle volumetric density (ρ_i, in kg/m^3) and size distribution, and r is the scattering ratio between the 89 GHz and 157 GHz channels. The parameters associated with the *IWP* calculation are: μ, ρ_i, $\Omega_{89or157}$ and Ω_N, which are the cosine of the zenith angle, ice particle volumetric density, scattering coefficient in both channels and the normalized

scattering coefficient, respectively. The empirical relation (Eq. (1)) between D_e and r is determined based on simulated data from a radiative transfer model (see Weng, 1992; Zhao and Weng, 2002). An ice particle volumetric density of 920 kg/m^3 has been used in the tropics for precipitating ice clouds (similar to that used by Atlas et al., 1995; Weng and Grody, 2000). Hydrometeors having such a density may originate as frozen large cloud droplets or raindrops. On the other hand, for snow, the density may be lower than 100 kg/m^3 (Hobbs et al., 1975) and, for graupel, above 500 kg/m^3 (Weng and Grody, 2000), and also depends on the ice size (Atlas et al., 1995). Thus, for a 30% uncertainty in the ice volumetric density value, the retrieval error of D_e ranges on average from 5% to 20%, depending on D_e, while the value alone would result in an error of 25% in the *IWP* (Zhao and Weng, 2002). The utilized regression coefficient values are shown in Table 1.

The 89 GHz channel is insensitive to signal scattering originating from small particles, thus the ratio between scattering coefficients at 89 GHz and 157 GHz expresses the scattering by larger particles. This ratio is expressed as

$$r = \frac{\Omega_{89}}{\Omega_{157}}, \tag{3}$$

where Ω_{89} and Ω_{157} are the scattering coefficients in the 89 GHz and 157 GHz channels, respectively. Based on a two stream approximation similar to that presented by Weng and Grody (2000), the scattering coefficient for both channels (Ω_{89} and Ω_{157}) is determined using the difference between the cloud base (T_b) and top (T_t) temperatures, normalized by the value of the cloud top temperature, expressed as

$$\Omega_{89\,or\,157} = \frac{T_{b_{(89or157)}} - T_{t_{(89or157)}}}{T_{t_{(89or157)}}}. \tag{4}$$

The cloud top brightness temperatures in both channels (T_{t89} and T_{t157}) are estimated from the NOAA-18 satellite and corrected considering the local zenith angle. On the other hand, cloud base temperatures (T_{b89} and T_{b157}) for the continent are estimated using the empirical relationship between the low frequencies (23 and 31 GHz) of the AMSU-A2 sensor and the high frequencies of the MHS sensor, as presented by Zhao and Weng (2002). This expression is defined as

$$T_{b89} = 17.88 + 1.61T_{t23} - 0.67T_{t31} \tag{5}$$

and

$$T_{b157} = 33.78 + 1.69T_{t23} - 0.80T_{t31}. \tag{6}$$

Table 1
Coefficients used to determine D_e and *IWP*.

	a_0	a_1	a_2	a_3
D_e	−0.3003	4.3088	−3.9826	2.7832
		b_0	b_1	b_2
IWP	$D_e \geq 1.0$ mm	−1.1930	2.0883	−0.8575
	$D_e < 1.0$ mm	−0.2945	1.3884	−0.7536

In this way, the empirical relation between D_e and r is used to determine the ice particle size, only considering values of the scattering coefficient (r) less than 0.8. Thus, the condition for a detectable cloud considers only temperatures at 183.3 GHz less than 265 K. For D_e less than (greater than) 1 mm, the $\Omega_{157}(\Omega_{89})$ is used in Eq. (2); μ (determined using the local zenith angle); D_e, and ρ_i (920 kg/m^3) are also used, while Ω_N is determined by

$$\Omega_N = \exp\left[b_0 + b_1\ln(D_e) + b_2(\ln(D_e))^2\right], \tag{7}$$

where b_0, b_1 and b_2 are the regression coefficients for the values of D_e above and below 1 mm. The coefficient values used for both classes of D_e are shown in Table 1.

The effects of image edge pixel deformation were eliminated using viewing angles (local zenith angle) between ±25° (Bennartz, 2000; Stubenrauch et al., 2004), considering that at the sub-satellite point (footprint), the spatial resolution is 20 km by 16 km. For each pixel, a search was made for CG lightning occurrences from 7.5 min before until 7.5 min after the time of the scanned line. Statistical analyses of dispersion and standard deviation associating D_e and *IWP* with CG lightning were conducted, evaluated with Pearson's correlation coefficients (R) and p-values (pv) with a significance level of 0.01.

The T_B from the 85 GHz channel with vertical (T_{BV}) and horizontal (T_{BH}) polarization from the TMI sensor on board the TRMM satellite were used to estimate the ice particle orientation. As discussed by some authors (Prigent et al., 2001; Prigent et al., 2005), the temperature difference (T_{BV}–T_{BH}) at 85 GHz can indicate the region and preferential orientation type (vertical or horizontal) of the ice particle associated with electrical activity. For the region and period of study cited earlier, only pixels with a Polarization Corrected Temperature (PCT) of less than 250 K were selected, in order to avoid signals not originating from convective clouds (similar to Spencer et al., 1989; Mohr et al., 1996; Mohr and Zipser, 1996; Cecil et al., 2002; Biscaro and Morales, 2008). Thus, for each pixel, the difference T_{BV}–T_{BH} was determined, and the lightning occurrences were counted from 7.5 min before until 7.5 min after the time of the scanned line, in an elliptical region of 7 km by 5 km centered at the pixel position. Statistical analyses similar to those discussed earlier for other parameters were also applied to the relationship of T_{BV}–T_{BH} with CG lightning occurrence.

3. Results

3.1. The diurnal cycle of the MCSs area expansion and convective fraction and CG lightning

The diurnal cycles of the physical properties were evaluated only for the moments of the life cycle when the systems were passing over the study region, considering only the cases without splits (division of systems) and merges (fusion of systems). The 16,520 MCSs identified over the area and during the analyzed period (2007–2009) presented 951,359 CG lightning occurrences. Fig. 2 shows the diurnal cycle of CG lightning occurrences (sum by hour of CG lightning occurrences associated with MCSs during the study period) and average CG

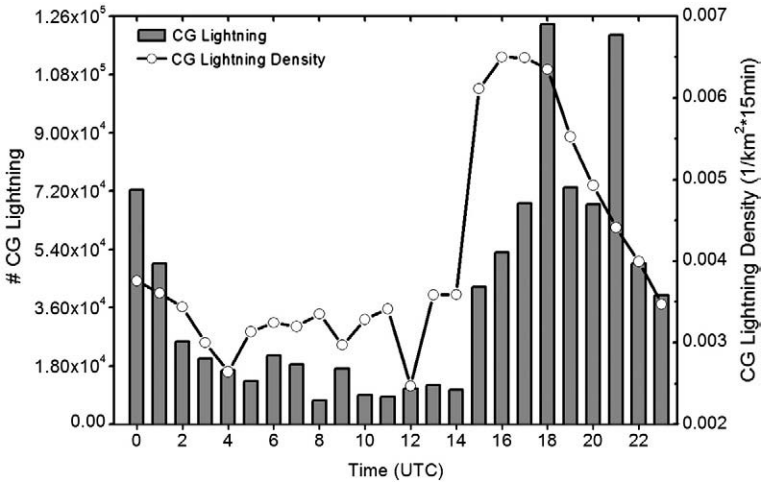

Fig. 2. Hourly CG lightning occurrences in convective systems and CG lightning density (CG lightning per MCSs area in 15 min intervals).

lightning density (# CG lightning/km^2*15 min). These CG lightning parameters exhibited a coherent and organized behavior, achieving maximum intensity during the afternoon and beginning of the night. Peak electrical activity was observed at 18 UTC and 21 UTC, while the minimum occurred at 8 UTC. The minimum lightning density was noted at 12 UTC, and in contrast, the maximum is reached 2 h before that of CG lightning occurrence, and is followed by a strong decrease in values. This diurnal cycle showed the modulation of convection forced by diurnal solar heating, while the delay of CG lightning occurrence relative to the lightning density indicates that shorter systems found before maturation are efficient lightning producers, even though maximum CG lightning occurrence occurs later. Similar results were also observed in the US (Orville et al., 2001), Austria (Schulz et al., 2005), Europe (Manoochehrnia et al., 2007) and Brazil (Pinto et al., 2003). However, the second peak of CG lightning occurrence at 21 UTC suggests the incursion of larger systems with a more nocturnal character, and can be associated with forcing from nocturnal cold fronts.

The physical properties of the diurnal cycle of storms and thunderstorms show a phased behavior, but with distinct intensity as observed in Fig. 3. The normalized area expansion (A_e, in $10^{-6}s^{-1}$) rate corresponds to the system size temporal variation rate between two consecutive images (during this study the time interval was 15 min) normalized by in the average area. The convective fraction (FC) represents the ratio between the number of pixels with $T_B<210$ K and $T_B<235$ K. It is noted that a stronger increase of A_e occurred after 12 UTC, reaching its maximum value at 15–16 UTC, followed by a rapid decrease. However, higher A_e values for thunderstorms indicate that lightning is located in progressively growing systems (that is, presenting only positive A_e values) and lower mass flow in storms is not favorable to initiation of cloud electrification. In comparison with Fig. 2, it is observed that during the diurnal cycle, A_e consistently

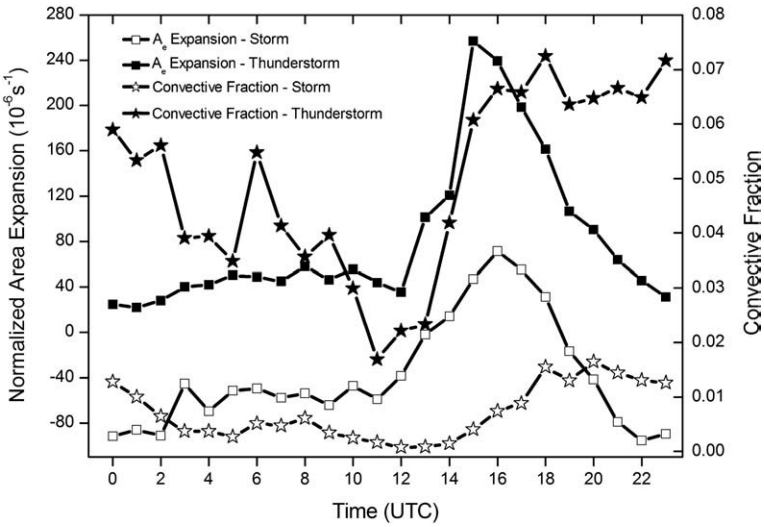

Fig. 3. Mean hourly normalized area expansion ($10^{-6}\,s^{-1}$) and convective fraction for storms and thunderstorms.

modulates CG lightning occurrence and hence an A_e maximum occurs 3 h before the moment of maximum CG lightning occurrence. This is the moment of system formation and development prior to the mature phase, in which convective processes are very intense. Since area expansion is associated with mass flux inside the cloud (Machado and Laurent, 2004), it is expected to be one of the moments of maximum convective system electrification. The FC of thunderstorms grows faster than that of storms, reaching its maximum at 18 UTC and sustaining intense convective cells after that point. The high FC values sustained after 18 UTC are consistent with the double peak electrical activity found in the results in Fig. 2. It is also noted that thunderstorms present maximum convective activity before storms, while for both, the maximum FC region occurs after the A_e maximum. In this way, it is noted that the existence of the largest convective fractions during the night, associated with a large number of electrical discharges, is probably due to systems of long duration that consequently attain large convective areas. These results indicate that the electrical activity density is highest at the moment when the clouds are growing and have the most intense convective cells, and that the largest number of electrical discharges occurs when the system is close to maturation, attaining the largest convective area.

3.2. Relationship of convective system area and temperature with CG lightning

The analysis of MCSs physical properties evaluated the relationship of cloud horizontal dimension (dynamical aspect) and top height (thermodynamic aspect) with CG lightning occurrence. Fig. 4 presents the average number of CG lightning (# CG lightning per MCSs in 15 min intervals) and the associated standard deviation as a function of the effective radius (km) of the system. The effective radius corresponds to the radius of a circle with an equal area to that of the MCSs. The MCSs area corresponds to a cluster larger than 90 pixels (1440 km^2) and with an average temperature below 235 K (Machado et al., 1998; Vila et al., 2008). A rapid linear growth in the area is associated with a strong increase in electrical activity (as noted in the high correlation coefficient $R=0.96$, $pv=9.63\times10^{-11}$). An average increase in radius of 100 km results in an increase of approximately 140 CG lightning for systems smaller than 200 km. However, this relationship is valid on average, and only considers the factor of the cloud cluster area, while it is evidenced in the literature that electrical activity is dependent on a complex combination of physical and microphysical characteristics. It is interesting to note that a recent and completely independent study (Altaratz et al., 2010) found a more intense production of return strokes associated with the largest cloud cover over the Amazon region. Consistent with the findings of this study, these large areas are associated with strong high level wind divergence, which is due in part to intense updrafts (mass flux) in deep convective clouds, capable of sustaining and intensifying the mutual interaction of ice particles involved in the electrification process. These dynamical characteristics of mesoscale cloud organization have also been observed in studies such as Machado and Laurent (2004) for the Amazon region and Tadesse and Anagnostou (2009) for the US.

Fig. 5 shows the average relationship of the number of CG lightning (# CG lightning per MCSs in 15 min intervals) with the minimum cloud top temperature (K) and the corresponding cloud top height (km). In this case, the temperature corresponds to the average of the coldest pixels nine temperatures those belonging to the convective towers embedded in the interior of the MCSs. The cloud top height was estimated supposing a cloud emissivity equal to 1 and a standard tropical atmosphere (Thomas and Stamnes, 1999). In this figure, it can be noted that the clouds with the highest tops (lowest brightness temperature) are strongly correlated ($R=0.84$, $pv=1.24\times10^{-6}$) with the regions with the most electrical activity. These clouds are associated with deep convection able to penetrate the tropopause (15–16 km) and

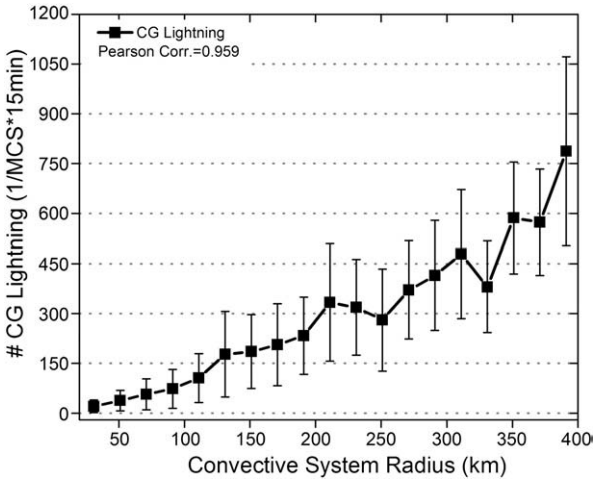

Fig. 4. Average and standard deviation of CG lightning occurrence per convective system in 15 min intervals (#CG lightning/MCSs*15 min) as a function of the effective radius (km).

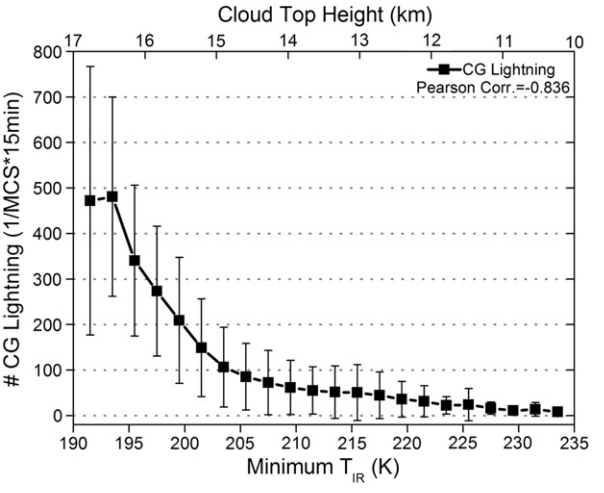

Fig. 5. Average and standard deviation of CG lightning occurrence per convective system in 15 min intervals (#CG lightning/MCSs*15 min) as a function of the IR Minimum Temperature (K) and cloud top height (km).

create favorable conditions for cloud electrification, as discussed by Machado et al. (2009). Some of the qualitative similarities of these results have been observed in various studies. In agreement, the results of Williams (1985) and Ushio et al. (2001) suggested a nonlinear relationship between lightning and cloud top height, while, in support of these observations, Goodman et al. (1988) and Scofield et al. (2005) verified intense electrical activity for the lowest cloud top temperatures. Although the temperature thresholds were found to be different in diverse regions (which could be associated with local meteorological conditions, tropopause height or the conditions for the definition of the systems), in general, an intensification of the electrification processes by the deepest clouds has been a common observed feature.

The results indicate that there is a combined effect of regions of intense deep clouds with the lowest temperatures and strongest vertical velocities. These aspects show the influence of large areas with mixed phase hydrometeors that can lead to the formation of an intense charge center and trigger lightning. Another important aspect is that only temperatures below 210 K (cloud height above 14 km) are characterized by a significant increase in the average electrical activity growth rate. For values above this threshold, the relationship has a low significance and is approximately linear. This is an indication that this region could be associated with areas with the most intense cold tops, which could possibly result in thermodynamic conditions more favorable to intensive production of ice particles (Wallace and Hobbs, 1977). The largest standard deviations for the lowest temperatures are associated with the few events in this class range.

3.3. Convective system life cycle characteristics

For the analyzed period (May 2007 to August 2009) and region, and considering the limitations previously discussed, from a total of 16,520 MCSs life cycles, only 720 systems satisfied the requirements of having passed over the target area, having few missing images and not having initiated or dissipated as merge and split cases. Among the systems tracked and identified by the ForTraCC algorithm, a total of 420 presented at least one CG lightning during their life cycle, while in 300 systems no CG lightning occurrences were detected. The differences between storms and thunderstorms are, however, initially analyzed in terms of the total life cycle duration. Fig. 6a and b show the accumulated and relative frequency distribution (in percentage) of total duration of systems without and with CG lightning, respectively. For both groups of systems, those with shorter duration predominate, which was to be expected since there is an almost linear relationship between size and duration, with smaller ones (or those with shorter duration) much more numerous than larger ones (or those with longer duration). However, the characteristic that is highlighted in these results is that the duration of the thunderstorms (at the 90% level) is on average one hour longer than that of the storms. It is noted that 26% of the storms have duration of less than 1.5 h, while this is true for only 16% of the thunderstorms. The longer duration of the thunderstorms in relation to the storms suggests the existence of more vigorous convection during the initial stages, sustaining the systems for a longer period. This indicates that the dynamic forcing during the system initiation stage is important for the intensification of convection and the charging processes inside the cloud.

The MCSs life cycle can be classified through the area evolution as initiation (first time detected), mature (maximum area) and dissipation (last time detected) stages. The variation of average area (effective radius in km) throughout the life cycle of storms and thunderstorms with total duration of 1–5 h is shown in Fig. 6c and d, respectively. The area increases rapidly during the first life stages, growing at a slower rate until reaching maturation at close to the half life of the systems, followed by strong area decay during the dissipation stage. Another commonly observed aspect is that the systems with a longer duration simultaneously present larger areas throughout the life cycle and a more intense initial area expansion. The works of Machado and Laurent (2004) and Tadesse and Anagnostou (2009) also suggested that the area growth rate during the initial stage is a parameter indicative of the degree of convection severity. On the other hand, the thunderstorms present a larger initial area expansion and the largest areas during the lifetime evolution. For an average lifetime of 4 h, the systems with lightning present an average initial expansion three times larger in relation to the storms with the same duration and two times less intense than those with 5 h of duration from the same group of thunderstorms. This analysis suggests that the initial stage of the thunderstorms is composed of more intense updrafts capable of creating clouds with higher tops and a larger liquid water content, which can intensify convective activity and consequently lightning occurrence.

Fig. 7a presents the evolution throughout the MCSs life cycle of average CG lightning occurrence (# CG lightning per MCSs in 15 min intervals) and effective radius (km) for five life cycle stages: initiation — the first time that the system was detected (stage 1); the intermediate stage between initiation and maturation (stage 2); maturation — maximum size (stage 3); intermediate between maturation and dissipation (stage 4) and dissipation — the last time that the system was detected (stage 5). The period of most intense electrical activity is found between initiation and maturation (50% of the entire CG lightning occurrence is found between stages 1 and 2 and 80% before maturation), while a less pronounced lightning occurrence is observed after this stage (less than 20% of the lightning occurred during the last two stages). It is noted that a strong increase in lightning occurrence and MCSs area occurs during the first two life cycle stages. The maximum lightning occurrence is observed in stages 2 and 3, while 33% of the occurrences are observed solely in the mature phase. A rapid decrease in electrical activity is observed in phases 4 and 5, probably due to the weakening of convective processes in the dissipation stage. Parker et al. (2001) found a maximum of both positive and negative CG lightning close to maturation, and the same has been observed in analyses of lightning (Goodman and MacGorman, 1986; Tadesse and Anagnostou, 2009). A similar behavior (Fig. 7b) of the evolution of the average number of CG lightning per MCSs in 15 min intervals is observed for discrete MCSs lifetimes from 1 to 4 h. This result suggests that the longer the MCSs life cycle duration, the later the maximum electrical activity occurs, between the initiation and maturation stages. Based on these results, the most intense electrical activity during the initial stages is associated with a high

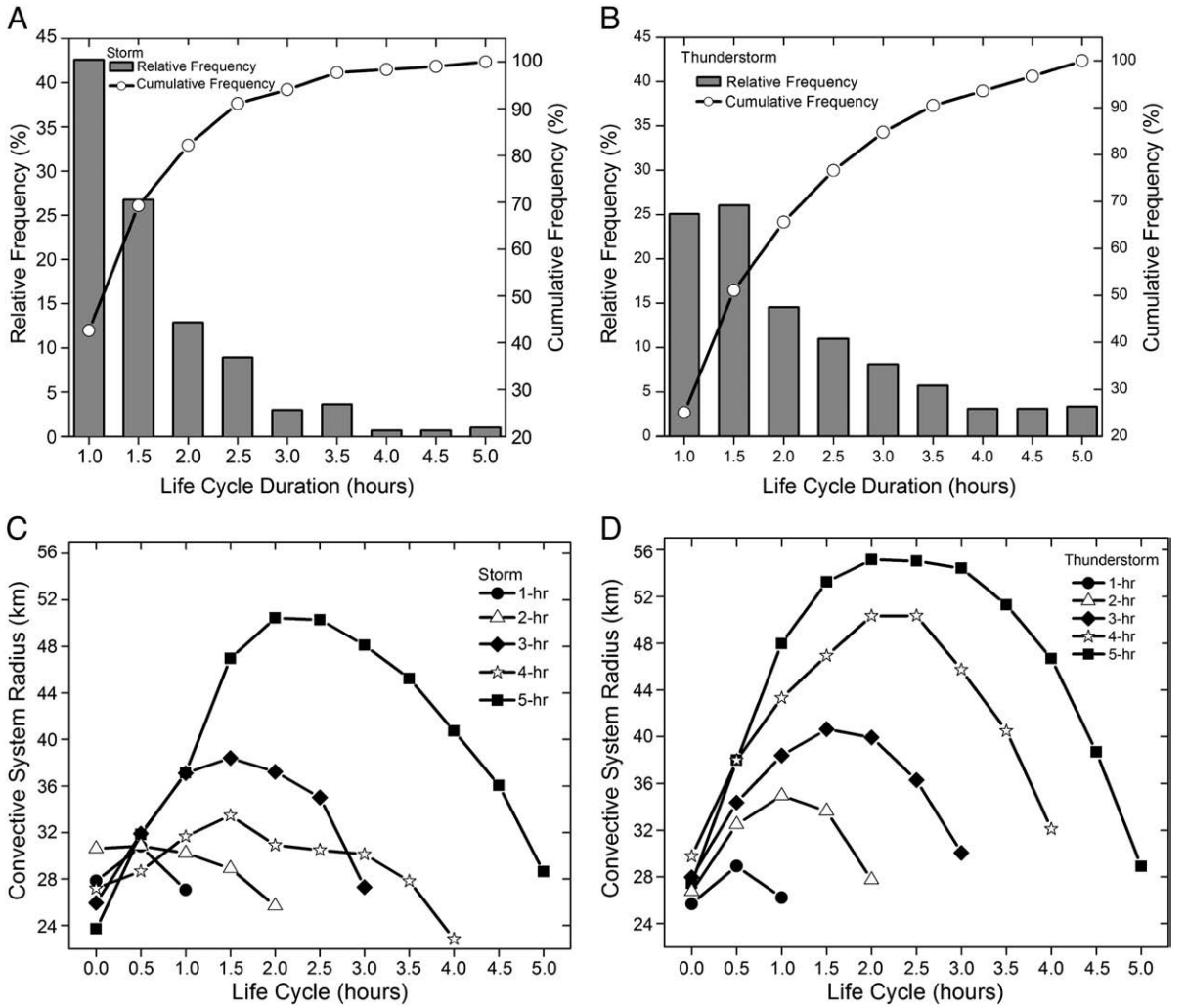

Fig. 6. The relative and cumulative frequency (%) distribution of the life cycle duration of (A) storms and (B) thunderstorms and average convective system effective radius (km) over the life cycle of (C) storms and (D) thunderstorms for systems with duration between 1 and 5 h.

condensation rate, combined with intense mass flux and MCSs area growth. Indeed, it is during this stage that the systems minimum brightness temperatures and maximum convective cell areas are observed (Machado et al., 1998). The formation and interaction of ice particles is enabled during these stages, leading to a more intense electrification process.

Complementing the results mentioned, the maximum CG lightning density (number of CG lightning per km^2 in 15 min intervals) occurs during the initiation phase (Fig. 7c). The same is observed for discrete lifetime values of CG lightning density, as shown in Fig. 7d. In agreement, it can also be noted that the shorter the MCSs lifetime, the more quickly the electrical activity maximum is obtained. The high electrical discharge density in the first stages indicates that the convection process during this stage is more localized. As the MCSs evolves, it becomes composed of a large quantity of cirrus and stratiform clouds, which are much less efficient in producing electrical discharges. During dissipation, the systems decrease in size and fragment; however, the convection is much less intense, naturally leading to lower electrical activity.

3.4. Microphysical proprieties

As previously discussed, the analysis of the D_e and *IWP* parameters considered only pixels with local zenith angle between $\pm 25°$ over the study region and during the period from January 2007 to September 2009. This resulted in the identification of approximately 6027 events (number of NOAA pixels) associated with a 35,811 CG lightning occurrences. Fig. 8 shows the average behavior of the CG lightning occurrences per pixel in 15 min intervals (# CG lightning/pixel*15 min) as a function of the ice particle effective diameter (D_e, in mm). In general, an increase in the average occurrence of CG lightning is associated with an increment in ice particle size, as shown by the high Pearson's correlation ($R = 0.86$, $pv = 2.11 \times 10^{-6}$). However, a relationship between these two variables is only noted for D_e greater than 1 mm. In agreement with these results, Zhao and Weng (2002) found that the largest ice particles (diameter between 0.9 and 1.2 mm) were located in the most intense convective regions of mid-latitude storms, while Keith and Saunders

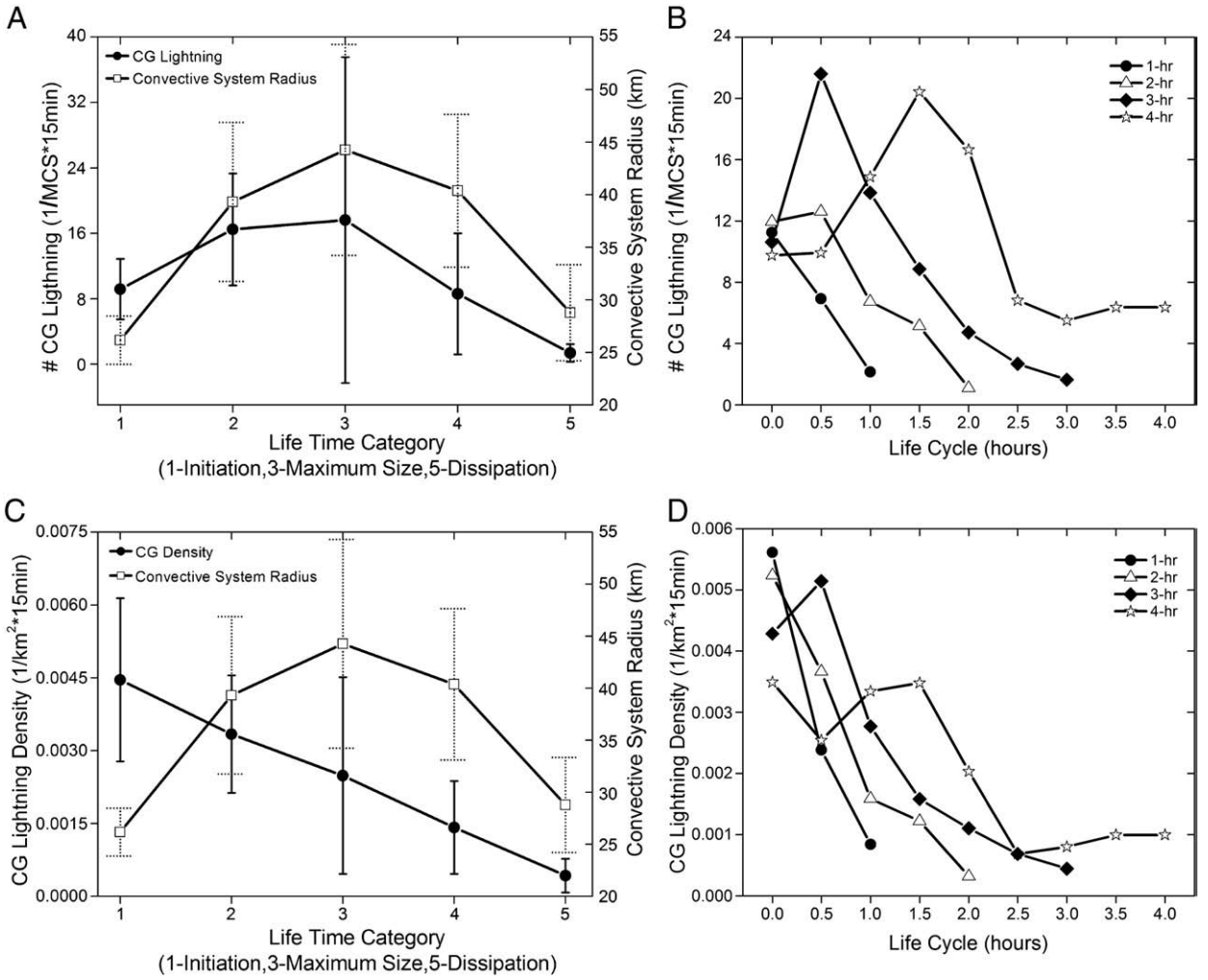

Fig. 7. Average (A) CG lightning occurrence (# CG lightning/MCS*15 min) for five categories of the convective system life cycle (1-Initiation, 2-Intermediate stage between initiation and mature stage, 3-Mature stage (maximum size stage), 4-Intermediate stage between the mature and dissipation stage, and 5-Dissipation stage), and (B) CG lightning occurrences for convective systems having a duration between 1 and 4 h. Similarly, sub-figures C and D present the average CG lightning density (# CG lightning density/km^2*15 min).

(1990) verified a nonlinear dependence on the quantity of charge transferred between particles with this size. This suggests that ice particles smaller than 1 mm do not have a sufficient contact area during the collisions to lead to an efficient charge transfer. The decrease in lightning occurrence for ice particle diameters greater than 1.6 mm and with high standard deviation values can be attributed to large ice particles not associated with active convective clouds, yet the small number of observed events in these classes does not permit the extraction of precise information.

Average lightning electrical activity (# CG lightning/pixel*15 min) varies with the *IWP* in an approximately linear form ($R=0.96$, $pv=3.49\times10^{-12}$), as shown in Fig. 9. An increase in ice content of 0.5 kg m^{-2} represents an average increase of six CG lightning. Similar results have been observed correlating total lightning (IN + CG) data originating from LIS and TMI (Baker et al., 1995; Blyth et al., 2001). These results indicate that the larger availability of ice particles in the cloud interior could intensify the collision rate, leading to a larger quantity of electrified particles and intensifying the electrification process. Nevertheless, it is noted that the *IWP* can play an important role in other forms of electric charge transfer during the collisions. Strong electrical activity occurs for a large range of *IWP* values, while for the D_e analyses this only occurs above a threshold. This suggests that ice content is important during the occurrence of lower electrical activity rates, while for the largest convection intensities, D_e has a slightly more effective role.

The analysis of the interdependence of electrical activity with ice particle polarization identified 13,207 events (number of TRMM-TMI pixels) associated with 37,302 CG lightning occurrences. Thunderstorms possess important peculiarities in relation to the preferential ice particle orientation in their interior, which can be revealed by the polarization difference in the 85 GHz channel (T_{BV}–T_{BH}). The decrease in the polarization difference (more negative differences, that is, those associated with regions with

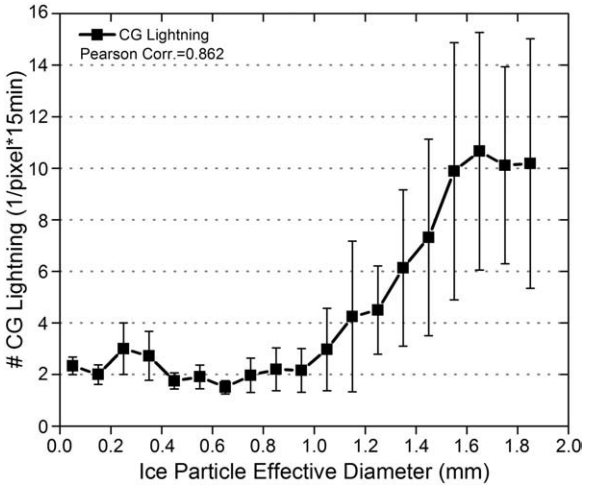

Fig. 8. Average and standard deviation of CG lightning occurrence in 15 min intervals by pixel (# CG lightning/pixel * 15 min) as a function of ice particle effective diameter (mm).

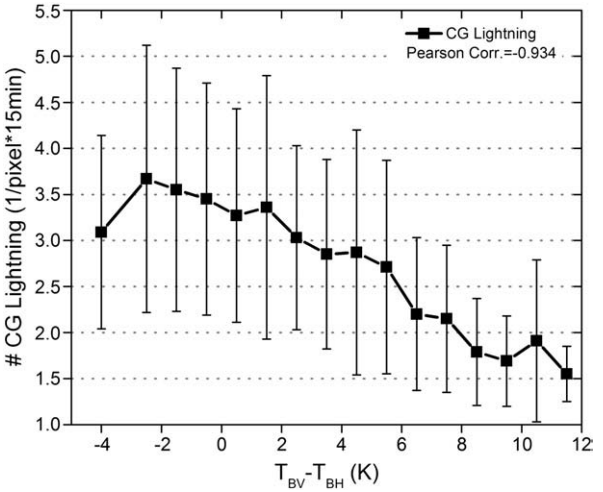

Fig. 10. Average and standard deviation of CG lightning occurrence in 15 min intervals by pixel (# CG lightning/pixel * 15 min) as a function of the Polarized Temperature Difference at 85 GHz (T_{BV}–T_{BH}).

vertically oriented particles) is associated with a large increase in the number of CG lightning events (Fig. 10). Indeed, these characteristics are also revealed by the high correlation coefficient ($R=0.93$, $pv=1.18\times10^{-7}$), which demonstrates that intense convective centers are capable of attenuating vertically polarized radiation in a more efficient manner. Previous studies have also observed this characteristic for total lightning (IN + CG) (Prigent et al., 2005), as well as for only CG lightning (Spencer et al., 1989). The explanation consists of the existence of strong updrafts and an intense vertical electric field capable of aligning ice particles preferentially in the vertical. This orientation is capable of more effectively attenuating the vertically polarized signal, as opposed to that propagating in the horizontal direction. Thus, these results indicate that a combination of information at 85 GHz (vertical and horizontal polarization) channel and electrical activity could provide a reasonable approximation of the location and preferential symmetry axis orientation of these particles, and consequently identify regions more suitable for triggering of lightning.

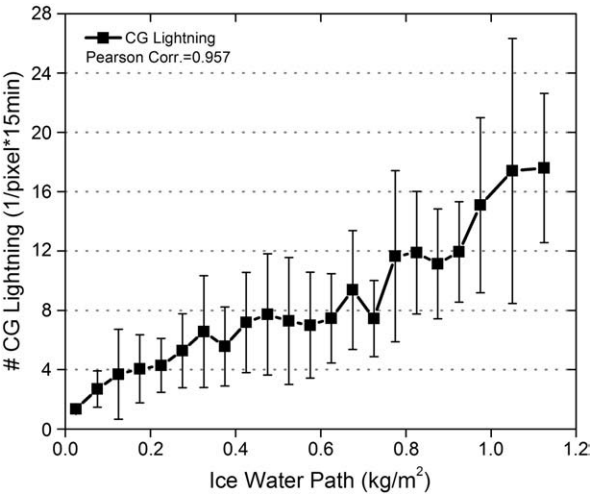

Fig. 9. Average and standard deviation of CG lightning occurrence in 15 min intervals by pixel (# CG lightning/pixel * 15 min) as a function of Ice Water Path (kg/m^2).

4. Conclusions

This study combined information originating from infrared and microwave channels with CG lightning occurrence in order to evaluate the relationship between physical and microphysical properties and electrical activity in Mesoscale Convective Systems (MCSs). An automatic MCSs tracking method was applied over an area with a CG lightning detection efficiency consistently above 90% in the period from 2007 to 2009. The diurnal cycle analysis showed an electrical activity maximum close to the time of maximum convective fraction and 3 h after the maximum area expansion rate. It was also concluded that the area expansion can be used as an indicator parameter of maximum lightning density during the diurnal cycle. The maximum lightning density occurs a few hours before the maximum CG lightning occurrence, since the maximum is also associated with the development of a larger convective area. Among the evaluated physical properties, the size and minimum brightness temperature of the MCSs showed the strongest correlations with the convection intensity and the CG lightning frequency. This suggests that the updraft intensities and the heights of the convective towers embedded in these systems are relevant parameters for the identification of thunderstorm severity and immediate weather prediction.

The initial area expansion was shown to be an important parameter for defining the development stage and the potential of the systems to produce electrical activity. The thunderstorms showed a well-defined life cycle in relation to the storms, with a longer lifetime and larger area. The maximum lightning frequency occurs during the growth phase close to maturation, while the average lightning density maximum is attained during the first life cycle stages. Lower electrical activity intensity was observed after achieving maturation. The physical

explanation for these results is based on the combination of the intense condensation rate and mass flux during the development of the systems, enabling an intensification of the convective cloud electrification processes and a later increase in MCSs convective area, which also occurs for other cloud types, some of which were unable to develop electrical activity.

The ice size and content showed a strong positive correlation with CG lightning, as was also found in previous studies for other regions. These results demonstrate that a high availability of the largest ice particles is a relevant microphysical characteristic for the formation of intense charge centers and the initiation of electrical activity. A significant increase in electrical activity was observed only for ice particles larger than 1 mm. The polarization difference at 85 GHz showed potential as a technique for identifying regions of more intense convection associated with ice particles preferentially oriented in the vertical.

The analyses demonstrated that aspects such as MCSs size and minimum brightness temperature, combined with information about cloud microphysics, could be useful parameters for immediate prediction of electrical activity and diagnosis of thunderstorm severity. Assimilation of microphysical parameters in synergy with lightning occurrence in medium-term prediction models could also provide relevant additional information. Future plans are to expand these results to other seasons and continental regions of Brazil, but first it will be necessary to increase the BrasilDAT network in this region. Moreover, additional information about cloud electrification processes and the thunderstorm life cycle may be obtained through consistent analysis of polarity (positive and negative CG lightning), electrical current peak and flash multiplicity and total lightning (intra-cloud + cloud-to-ground) for MCSs. Thus, the physical and microphysical processes involved in cloud electrification and lightning occurrence are shown to be extremely complex and dependent on numerous variables. However, a set of cloud physical parameters could provide new tools for monitoring and forecasting of electrical discharge in MCSs, and is important background information for understanding cloud processes.

Acknowledgments

The authors thank NOAA for providing the satellite data and BrasilDAT for the CG lightning information. The first author was financed with a graduate fellowship from CAPES (Coordination for the Improvement of Higher Level Personnel) during the completion of a master's degree in Atmospheric Sciences at INPE.

References

Altaratz, O., Koren, I., Yair, Y., Price, C., 2010. Lightning response to smoke from Amazonian fires. Geophys. Res. Lett. 37 (1–6), L07801. doi:10.1029/2010GL042679.

Anderson, C.J., Arritt, R.W., 1998. Mesoscale Convective Complexes and persistent elongated Convective Systems over the United States during 1992 and 1993. Mon. Weather Rev. 126, 578–599.

Ashley, W.S., Mote, T.L., Dixon, P.G., Trotter, S.L., Powell, E.J., Durkee, J.D., Grundstein, A.J., 2003. Distribution of Mesoscale Convective Complex rainfall in the United States. Mon. Weather Rev. 131, 3003–3017.

Atlas, D., Matrosov, S.Y., Heymsfield, A.J., Chou, M.D., Wolf, D.B., 1995. Radar and radiation properties of ice clouds. J. Appl. Meteorol. 34, 2329–2345.

Baker, M.B., Dash, J.G., 1989. Charge transfer in thunderstorms and the surface melting of ice. J. Cryst. Growth 97, 770–776.

Baker, M.B., Christian, H.J., Latham, J., 1995. A computational study of the relationships linking lightning frequency and other thundercloud parameters. Q. J. R. Meteorol. Soc. 121, 1525–1548.

Bateman, M.G., Rust, W.D., Smull, B.F., Marshall, T.C., 1995. Precipitation charge and size measurements in the stratiform region of two Mesoscale Convective Systems. J. Geophys. Res. 100 (D8), 341–356. doi:10.1029/95JD01280.

Bennartz, R., 2000. Optimal convolution of AMSU-B to AMSU-B. J. Atmos. Oceanogr. Technol. 17, 1215–1225.

Biscaro, T.S., Morales, C.A., 2008. Continental passive microwave-based rainfall estimation algorithm: application to the Amazon Basin. J. Appl. Meteorol. Climatol. 47, 1962–1981. doi:10.1175/2007JAMC1744.1.

Bluestein, H.B., MacGorman, D.R., 1998. Evolution of cloud-to-ground lightning characteristics and storm structure in the Spearman, Texas, tornadic supercells of 31 May 1990. Mon. Weather Rev. 126, 1451–1467.

Blyth, A.M., Christian, H.J., Driscoll, K., Gadian, A.M., Latham, J., 2001. Determination of ice precipitation rates and thunderstorm anvil ice contents from satellite observations of lightning. Atmos. Res. 59–60, 217–229. doi:10.1016/S0169-8095(01)00117-X.

Bonner, W.D., 1968. Climatology of the low level jet. Mon. Weather Rev. 96, 833–850.

Brooks, I.M., Saunders, C.P.R., Mitzeva, R.P., Peck, S.L., 1997. The effect on thunderstorm charging of the rate of rime accretion by graupel. Atmos. Res. 43, 277–295. doi:10.1016/S0169-8095(96)00043-9.

Carvalho, L.M.V., Jones, C., Liebmann, B., 2002. Extreme precipitation events in southeastern South America and large-scale convective patterns in the South Atlantic Convergence Zone. J. Climate 15, 2377–2394.

Cecil, D.J., Zipser, E.J., Nesbitt, S.W., 2002. Reflectivity, ice scattering, and lightning characteristics of hurricane eyewalls and rainbands. Part I: quantitative description. Mon. Weather Rev. 130, 769–784.

Cohen, A.E., Coniglio, M.C., Corfidi, S.F., Corfidi, S.J., 2007. Discrimination of Mesoscale Convective System environments using sounding observations. Weather Forecast 22, 1045–1062.

Conforte, J.C., 1997. A study of Mesoscale Convective System over South America. PhD Thesis (in Portuguese), 140 pp. National Institute for Space Research (INPE), Sao Jose dos Campos, Brazil.

DeLonge, M.S., Fuentes, J.D., Chan, S., Kucera, P.A., Joseph, E., Gaye, A.T., Daouda, B., 2010. Attributes of Mesoscale Convective Systems at the land–ocean transition in Senegal during NASA African Monsoon Multidisciplinary Analyses 2006. J. Geophys. Res. 115, D10213. doi:10.1029/2009JD012518.

Dotzek, N., Rabin, R.M., Carey, L.D., MacGorman, D.R., McCormick, T.L., Demetriades, N.W., Murphy, M.J., Holle, R.L., 2005. Lightning activity related to satellite and radar observations of a Mesoscale Convective System over Texas on 7–8 April 2002. Atmos. Res. 76, 127–166.

Durkee, J.D., Mote, T.L., 2009. A climatology of warm-season Mesoscale Convective Complexes in subtropical South America. Int. J. Climatol. 30, 418–431. doi:10.1002/joc.1893.

Ferreira, R.N., Rickenbach, T.M., Herdies, D.L., Carvalho, L.M.V., 2003. Variability of South American convective cloud systems and tropospheric circulation during January–March 1998 and 1999. Mon. Weather Rev. 131, 961–973.

Fritsch, J.M., Kane Jr., R.J., Chelius, C.R., 1986. The contribution of Mesoscale Convective weather systems to the warm-season precipitation in the United States. J. Clim. Appl. Meteorol. 25, 1333–1345. doi:10.1175/1520-0450(1986)025.

Goodman, S.J., MacGorman, D.R., 1986. Cloud-to-ground lightning activity in Mesoscale Complexes Convective. Mon. Weather Rev. 114, 2320–2328.

Goodman, S.J., Buechler, D.E., Meyer, P.J., 1988. Convective tendency images derived from a combination of lightning and satellite data. Weather Forecast 3, 173–188.

Hobbs, P.V., Radke, L.F., Atkinson, D.G., 1975. Airborne Measurements and Observations in Cirrus Clouds. Tech. Rep. AFCRLTR-75–0249, Air Force Geophysics Laboratory, Hanscom AFB, MA, 117 pp.

Holle, R.L., Watson, A.I., López, R.E., MacGorman, D.R., Ortiz, R., William, D., 1994. The life cycle of lightning and severe weather in a 3–4 June 1985 PRE-STORM Mesoscale Convective System. Mon. Weather Rev. 122, 1798–1808.

Hunter, S.M., Schuur, T.J., Marshall, T.C., Rust, W.D., 1992. Electric and kinematic structure of the Oklahoma Mesoscale Convective System of 7 June 1989. Mon. Weather Rev. 120, 2226–2239.

Jain, A.R., Panwar, V., Mandal, T.K., Rao, V.R., Goel, A., Gautam, R., Das, S.S., Dhaka, S.K., 2010. Mesoscale convection system and occurrence of extreme low tropopause temperatures: observations over Asian summer monsoon region. Ann. Geophys. 28, 927–940.

James J.N., 1992. A Preliminary Study of Mesoscale Convective Complexes over the Mid-latitudes of Eastern Australia. Tech. Report. Bureau of Meteorology: Melbourne, 30, 29–30.

Kane Jr., R.J., Chelius, C.R., Fritsch, J.M., 1987. Precipitation characteristics of Mesoscale Convective weather systems. J. Clim. Appl. Meteorol. 26, 1345–1357.

Keighton, S.J., Bluestein, H.B., MacGorman, D.R., 1991. The evolution of a severe Mesoscale Convective System: cloud-to-ground lightning location and storm structure. Mon. Weather Rev. 119, 1533–1556.
Keith, W.D., Saunders, C.P.R., 1990. Further laboratory studies of the charging of graupel during ice crystal interactions. Atmos. Res. 25, 445–464. doi:10.1016/0169-8095(90)90028-B.
Laing, A.G., Fritsch, J.M., 1993a. Mesoscale Convective Complex in Africa. Mon. Weather Rev. 121, 2254–2263.
Laing, A.G., Fritsch, J.M., 1993b. Mesoscale Convective Complexes over the Indian monsoon region. J. Climate 6, 911–919.
Laing, A.G., Fritsch, J.M., 1997. The global population of Mesoscale Convective Complexes. Q. J. R. Meteorol. Soc. 123, 389–405.
Laing, A.G., Fritsch, J.M., 2000. The large-scale environments of the global populations of Mesoscale Convective Complexes. Mon. Weather Rev. 128, 2756–2776. doi:10.1175/1520-0493(2000)12.
Laing, A.G., Fritsch, J.M., Negri, A.J., 1999. Contribution of Mesoscale Convective Complexes to rainfall in Sahelian Africa: estimates from geostationary infrared and passive microwave data. J. Appl. Meteorol. 38, 957–964. doi:10.1175/1520-0450(1999)038.
Lima, K.C., Gomes, R.G., 2009. Detection of atmospheric electrical discharges in Convective Systems with data from Simepar. Braz. J. Geophys. 27, 5–16. doi:10.1590/S0102-261X2009000100001.
Liu, D., Feng, G., Wu, S., 2009. The characteristics of cloud-to-ground lightning activity in hailstorms over northern China. Atmos. Res. 91, 459–465. doi:10.1016/j.atmosres.2008.06.016.
MacGorman, D.R., Morgenstern, C.D., 1998. Some characteristics of cloud-to-ground lightning in Mesoscale Convective Systems. J. Geophys. Res. 103, 11–23. doi:10.1029/97JD03221.
Machado, L.A.T., Laurent, H., 2004. The Convective System area expansion over Amazonia and its relationships with Convective System life duration and high-level wind divergence. Mon. Weather Rev. 132, 714–725.
Machado, L.A.T., Duvel, J.-P.H., Desbois, M., 1993. Diurnal variations and modulation by Easterly Waves of the size distribution of Convective Cloud Clusters over West Africa and the Atlantic Ocean. Mon. Weather Rev. 121, 37–49.
Machado, L.A.T., Rossow, W.B., Guedes, R.L., Walker, A.W., 1998. Life cycle variations of Mesoscale Convective Systems over the Americas. Mon. Weather Rev. 126, 1630–1654.
Machado, L.A.T., Lima, W.F.A., Pinto Jr., O., Morales, C.A., 2009. Relationship between cloud-ground discharge and penetrative clouds: a multi-channel satellite application. Atmos. Res. 93, 304–309. doi:10.1016/j.atmosres.2008.10.003.
Maddox, R.B., 1980. Mesoscale Convective Complexes. Bull. Am. Meteorol. Soc. 61, 1374–1387.
Manoochehrnia, P., Rachidi, F., Rubinstein, M., Schulz, W., 2007. Lightning Statistics in Switzerland. Proceedings of the International Symposium on Lightning Protection, 9. Iguassu Foz, Brazil. 7 pp.
Marengo, J.A., Douglas, M.W., Dias, P.L.S., 2002. The South America low-level jet east of the Andes during the 1999 LBA-TRMM and LBA-WET AMC campaign. J. Geophys. Res. 107 (D20), 8079. doi:10.1029/2001JD001188.
Marengo, J.A., Soares, W.R., Saulo, C., Nicolini, M., 2004. Climatology of the low-level jet east of the Andes as derived from the NCEP–NCAR reanalyzes: characteristics and temporal variability. J. Climate 17, 2261–2280.
Mazur, V., Rust, W.D., 1983. Lightning propagation and flash density in Squall Lines as determined with radar. J. Geophys. Res. 88, 1495–1502. doi:10.1029/JC088iC02p01495.
Miller, D., Fritsch, J.M., 1991. Mesoscale Convective Complexes in the Western Pacific Region. Mon. Weather Rev. 119, 2978–2992.
Miller, K., Gadian, A., Saunders, C., Latham, J., Christian, H., 2001. Modeling and observations of thundercloud electrification and lightning. Atmos. Res. 58, 89–115. doi:10.1016/S0169-8095(01)00089-8.
Mitzeva, R., Saunders, C.P.R., 1990. Thunderstorm charging: calculations of the effect of ice crystal size and graupel velocity. J. Atmos. Terr. Phys. 52, 241–245. doi:10.1016/0021-9169(90)90090-A.
Mohr, K.I., Zipser, E.J., 1996. Defining Mesoscale Convective System by their 85-GHz ice-scattering signatures. Bull. Am. Meteorol. Soc. 77, 1179–1189.
Mohr, K.I., Toracinta, R., Zipser, E.J., Orville, R.E., 1996. A comparison of WSR-88D reflectivities, SSM/I brightness temperatures, and lightning for Mesoscale Convective Systems in Texas. Part II: SSM/I brightness temperatures and lightning. J. Appl. Meteorol. 35, 919–931. doi:10.1175/1520-0450(1996)035.
Morel, C., Senesi, S., 2002. A climatology of Mesoscale Convective Systems over Europe using satellite infrared imagery. II: characteristics of European Mesoscale Convective Systems. Q. J. R. Meteorol. Soc. 128, 1973–1995. doi:10.1256/003590002320603494.
Naccarato, K.P., Pinto Jr., O., 2009. Improvements in the detection efficiency model for the Brazilian lightning detection network (BrasilDAT). Atmos. Res. 91, 546–563. doi:10.1016/j.atmosres.2008.06.019.
Nesbitt, S.W., Zipser, E.J., Cecil, D.J., 2000. A census of precipitation features in the tropics using TRMM: radar, ice scattering, and lightning observations. J. Climate 13, 4087–4106.
Nicolini, M., Saulo, A.C., Torres, J.C., Salio, P., 2002. Enhanced precipitation over southeastern South America related to strong low-level jet events during austral warm season. Argentine Meteorol. Cent. J. 27, 59–69.
Nielsen, K.E., Maddox, R.A., Vasiloff, S.V., 1994. The evolution of cloud-to-ground lightning within a portion of the 10–11 June 1985 Squall Line. Mon. Weather Rev. 122, 1809–1817.
Orville, R.E., Huffines, G., Gammon, J.N., Zhang, R., Ely, B., Steige, S., Phillips, S., Allen, S., Read, W., 2001. Enhancement of cloud-to-ground lightning over Houston, Texas. Geophys. Res. Lett. 28, 2597–2600. doi:10.1029/2001GL012990.
Parker, M.D., Rutledge, S.A., Johnson, R.H., 2001. Cloud-to-ground lightning in Linear Mesoscale Convective Systems. Mon. Weather Rev. 129, 1232–1242.
Petersen, W.A., Rutledge, S.A., 1992. Some characteristics of cloud-to-ground lightning in tropical Northern Australia. J. Geophys. Res. 97, 553–560.
Petersen, W.A., Christian, H.J., Rutledge, S.A., 2005. TRMM observations of the global relationship between ice water content and lightning. Geophys. Res. Lett. 32, L14819. doi:10.1029/2005GL023236.
Pinto Jr., O., Pinto, I.R.C.A., Diniz, J.H., Cazetta Filho, A., Cherchiglia, L.C.L., Carvalho, A.M., 2003. A seven-year study about the negative cloud-to-ground lightning flash characteristics in Southeastern Brazil. J. Atmos. Sol. Terr. Phy. 65, 739–748.
Pinto Jr., O., Pinto, I.R.C.A., Naccarato, K.P., 2007. Maximum cloud-to-ground lightning flash densities observed by lightning location systems in the tropical region: a review. Atmos. Res. 84, 189–200. doi:10.1016/j.atmosres.2006.11.007.
Prigent, C., Pardo, J.R., Mishchenko, M.I., Rossow, W.B., 2001. Microwave polarized signatures generated within cloud systems: Special Sensor Microwave Imager (SSM/I) observations interpreted with radiative transfer simulations. J. Geophys. Res. Atmos. 106, 28,243–28,258. doi:10.1029/2001JD900242.
Prigent, C., Defer, E., Pardo, J.R., Pearl, C., Rossow, W.B., Pinty, J.P., 2005. Relations of polarized scattering signatures observed by the TRMM Microwave instrument with electrical processes in cloud systems. Geophys. Res. Lett. 32, L04810. doi:10.1029/2004GL022225.
Reynolds, S.E., Brook, M., Gourley, M.F., 1957. Thunderstorm charge separation. J. Meteorol. 14, 426–436.
Rodgers, D.M., Howard, K.W., Johnston, E.C., 1983. Mesoscale Convective Complexes over the United States during 1982. Mon. Weather Rev. 111, 2363–2369.
Rutledge, S.A., Lu, C., MacGorman, D.R., 1990. Positive cloud-to-ground lightning in Mesoscale Convective Systems. J. Atmos. Sci. 47, 2085–2100.
Salio, P., Nicolini, M., Zipser, E.J., 2007. Mesoscale Convective Systems over southeastern South America and their relationship with the South American low-level jet. Mon. Weather Rev. 135, 1290–1309.
Saunders, C.P.R., 1993. Review of thunderstorm electrification processes. J. Appl. Meteorol. 32, 642–655. doi:10.1175/1520-0450(1993)032.
Saunders, C.P.R., Keith, W.D., Mitzeva, R.P., 1991. The effect of liquid water on thunderstorm charging. J. Geophys. Res. 96, 007–017. doi:10.1029/91JD00970.
Schulz, W., Cummins, K., Diendorfer, G., Dorninger, M., 2005. Cloud-to-ground lightning in Austria: A 10-year study using data from a lightning location system. J. Geophys. Res. 110, D09101. doi:10.1029/2004JD005332.
Schwendike, J., Kalthoff, N., Kohler, M., 2010. The impact of Mesoscale Convective Systems on the surface and boundary-layer structure in West Africa: case-studies from the AMMA campaign 2006. Q. J. R. Meteorol. Soc. 136, 566–582. doi:10.1002/qj.599.
Scofield, R.A., Kuligowski, R.J., Qiu, S., 2005. Combining Lightning with Satellite Data for Analysis and Prediction. Proceedings of the Conference on Meteorological Applications of Lightning Data, San Diego, United States.
Spencer, R.W., Goodman, H.M., Hood, R.E., 1989. Precipitation retrieval over land and ocean with the SSM/I: identification and characteristics of the scattering signal. J. Atmos. Oceanogr. Technol. 6, 254–273. doi:10.1175/1520-0426(1989)006.
Stubenrauch, C.J., Eddounia, F., Rädel, G., 2004. Correlations between microphysical properties of large-scale semi-transparent cirrus and the state of the atmosphere. Atmos. Res. 72, 403–423. doi:10.1016/j.atmosres.2004.03.024.
Tadesse, A., Anagnostou, E.N., 2009. Characterization of warm season Convective Systems over US in terms of cloud to ground lightning, cloud kinematics, and precipitation. Atmos. Res. 91, 36–46. doi:10.1016/j.atmosres.2008.05.009.
Thomas, G.E., Stamnes, K., 1999. Radiative Transfer in the Atmosphere and Ocean, First Ed. Cambridge University Press, New York.
Tollerud, E.I., Collander, R.S., 1993. Mesoscale Convective Systems and Extreme Rainfall in the Central United States. Proceedings of the Yokohama Symposium: Extreme Hydrological Events: Precipitation, Floods and Droughts, IAHS Publ., 213, pp. 11–19. Yokohama, Japan.

Torres, J.C., Nicolini, M., 1999. Analysis of a Mesoscale Convective System centered over the Río de la Plata. Aust. Meteorol. Mag. 48, 261–272.
Tsenova, B., Mitzeva, R., Saunders, C., 2009. A modeling study of the effect of ice particle sizes and relative velocity on ice crystal/graupel collisional charge transfer. Atmos. Res. 91, 250–258. doi:10.1016/j.atmosres.2008.04.008.
Ushio, T., Heckman, S.J., Boccippio, D.J., Christian, H.J., Kawasaki, Z.I., 2001. A survey of thunderstorm flash rates compared to cloud top height using TRMM satellite data. J. Geophys. Res. 106, 89–95. doi:10.1029/2001JD900233.
Velasco, I., Fritsch, J.M., 1987. Mesoscale Convective Complexes in the Americas. J. Geophys. Res. 92, 9591–9613.
Vera, C., Baez, J., Douglas, M., Emmanuel, C.B., Marengo, J.A., Meitin, J., Nicolini, M., Nogues-Paegle, J., Paegle, J., Penalba, O., Salio, P., Saulo, C., Silva, D.M.A., Dias, P.S., Zipser, E., 2006. The South American low-level jet experiment. Am. Meteorol. Soc. 87, 63–77.
Vila, D.A., Machado, L.A.T., Laurent, H., Velasco, I., 2008. Forecast and tracking the evolution of cloud clusters (ForTracCC) using satellite infrared imagery: methodology and validation. Weather Forecast 23, 233–245.
Wallace, M.J., Hobbs, V.P., 1977. Atmospheric Science: An Introductory Survey, First Ed. Academic Press, San Diego.
Weng, F., 1992. A multi-layer discrete-ordinate method for vector radiative transfer in a vertically-inhomogeneous, emitting and scattering atmosphere—I. Theory. J. Quant. Spectrosc. Ra. 47, 19–33. doi:10.1016/0022-4073(92)90076-G.
Weng, F., Grody, N.C., 2000. Retrieval of ice cloud parameters using a microwave imaging radiometer. J. Atmos. Sci. 57, 1069–1081.
Williams, E.R., 1985. Large-scale charge separation in thunderclouds. J. Geophys. Res. 90, 6013–6025. doi:10.1029/JD090iD04p06013.
Williams, E.R., Weber, M.E., Orville, R.E., 1989. The relationship between lightning type and convective state of thundercloud. J. Geophys. Res. 94, 213–220. doi:10.1029/JD094iD11p13213.
Zhao, L., Weng, F., 2002. Retrieval of ice cloud parameters using the advanced microwave sounding unit. J. Appl. Meteorol. 41, 384–395.
Zhou, Y., Qie, X., Soula, S., 2002. A study of the relationship between cloud-to-ground lightning and precipitation in the convective weather system in China. Ann. Geophys. 20, 107–113.
Zipser, E.J., Cecil, D.J., Liu, C., Nesbitt, S.W., Yorty, D.P., 2006. Where are the most intense thunderstorms on Earth? Bull. Am. Meteorol. Soc. 87, 1057–1071. doi:10.1175/BAMS-87-8-1057.